Published online 1 August 2012 *Nucleic Acids Research, 2012, Vol. 40, No. 19* **9633–9646**
doi:10.1093/nar/gks713

Meiotic DNA joint molecule resolution depends on Nse5–Nse6 of the Smc5–Smc6 holocomplex

Sophie Wehrkamp-Richter[1], Randy W. Hyppa[2], John Prudden[1], Gerald R. Smith[2,*] and Michael N. Boddy[1,*]

[1]Department of Molecular Biology, The Scripps Research Institute, La Jolla, CA 92037 and [2]Division of Basic Sciences, Fred Hutchinson Cancer Research Center, 1100 Fairview Avenue North, PO Box 19024, Seattle, WA 98109-1024, USA

Received April 25, 2012; Revised June 29, 2012; Accepted July 2, 2012

ABSTRACT

Faithful chromosome segregation in meiosis is crucial to form viable, healthy offspring and in most species, it requires programmed recombination between homologous chromosomes. In fission yeast, meiotic recombination is initiated by Rec12 (Spo11 homolog) and generates single Holliday junction (HJ) intermediates, which are resolved by the Mus81–Eme1 endonuclease to generate crossovers and thereby allow proper chromosome segregation. Although Mus81 contains the active site for HJ resolution, the regulation of Mus81–Eme1 is unclear. In cells lacking Nse5–Nse6 of the Smc5–Smc6 genome stability complex, we observe persistent meiotic recombination intermediates (DNA joint molecules) resembling HJs that accumulate in *mus81Δ* cells. Elimination of Rec12 nearly completely rescues the meiotic defects of *nse6Δ* and *mus81Δ* single mutants and partially rescues *nse6Δ mus81Δ* double mutants, indicating that these factors act after DNA double-strand break formation. Likewise, expression of the bacterial HJ resolvase RusA partially rescues the defects of *nse6Δ*, *mus81Δ* and *nse6Δ mus81Δ* mitotic cells, as well as the meiotic defects of *nse6Δ* and *mus81Δ* cells. Partial rescue likely reflects the accumulation of structures other than HJs, such as hemicatenanes, and an additional role for Nse5–Nse6 most prominent during mitotic growth. Our results indicate a regulatory role for the Smc5–Smc6 complex in HJ resolution via Mus81–Eme1.

INTRODUCTION

The repair of DNA damage by homologous recombination (HR) is central to the faithful propagation of chromosomes during both the mitotic and meiotic cycles. During mitotic growth, exogenous or endogenous genotoxic agents can induce DNA double-strand breaks (DSBs), which may also arise from replication fork mishaps [reviewed in (1)]. The HR-based repair of these insidious forms of DNA damage is executed by a relatively well-defined and largely overlapping set of proteins. Broken DNA ends are first resected to generate a single-stranded (ss) 3′-overhang, which acts as a platform for the subsequent homology search and invasion steps of HR [reviewed in (2)]. The ss DNA-binding protein complex replication protein A initially coats the 3′-overhang, which is subsequently displaced by loading of the RecA homolog Rad51, also called Rhp51 in fission yeast, as well as Dmc1 during meiosis (3–5). The Rad51 nucleoprotein filament invades a homologous duplex, forming a displacement loop (D-loop) that is used to prime repair synthesis and, at a broken fork, to restart replication. Meiotically induced Rec12 (Spo11 homolog) and several partner proteins form DSBs during fission yeast meiosis, to form crossovers important for the proper segregation of homologs at the first meiotic division (6,7). Genomic regions that are hotspots for meiotic DSB formation by Rec12 require Rad51 for DSB repair and recombination; in regions with lower DSB levels, both Rad51 and Dmc1, a meiosis-specific paralog, are required (3–5).

Following D-loop formation, there are various postulated pathways for the completion of DSB repair. A major pathway, thought to be essential for crossover formation, requires the processing of four-way DNA junctions called Holliday junctions (HJs (8–11)). The nature of the initiating lesion and whether the cell is in mitosis or

*To whom correspondence should be addressed. Tel: +1 858 784 7042; Fax: +1 858 784 2265; Email: nboddy@scripps.edu
Correspondence may also be addressed to Gerald R. Smith. Tel: +1 206 667 4438; Fax: +1 206 667 6497; Email: gsmith@fhcrc.org

The authors wish it to be known that in their opinion the first two authors should be regarded as the joint First Authors.

meiosis influence the mode of HJ processing. Closely spaced double HJs may be dissolved by the concerted action of a RecQ-related helicase and a topoisomerase partner (e.g. Sgs1–Top3 in budding yeast (12)). Notably, in fission yeast, the restart of broken replication forks critically depends on Mus81–Eme1 but not on the dissolution activity of Rqh1 (Sgs1 homolog)–Top3 (13). This likely reflects the formation of single, not double, HJs (or an HJ precursor) during restart of replication (12), because single HJs cannot be dissolved by a helicase and topoisomerase. Endonucleolytic HJ resolution facilitates crossing over between homologous chromosomes (homologs) and dominates during meiosis (8,14,15), when single HJs accumulate in *mus81* mutants (8,15). Dissolution of double HJs without associated crossover seems to be the major pathway in mitotic cells of some species (12) and seems to play a role during meiosis in budding yeast (16).

HJs arising through HR-mediated DSB repair can be resolved by endonucleolytic activities such as Mus81–Eme1 ((8,15–19)), Slx1–Slx4 (20,21)) and Yen1 (19,22). Recently, it was shown in the budding yeast *Saccharomyces cerevisiae* that Mus81–Mms4 and Yen1 endonucleases collaborate during meiosis to resolve HJs and that their activity is carefully regulated during the cell cycle (19). Mms4 (Eme1 homolog) is phosphorylated and then hyperactivated during meiosis I, whereas Yen1 activity is inhibited until meiosis II.

Mus81–Eme1 is critical in the fission yeast *Schizosaccharomyces pombe* where it is the only known complex involved in meiotic HJ resolution (8,15,23). A Yen1 ortholog has not been identified in the *S. pombe* genome, and Slx1–Slx4 has no detectable defect in meiotic recombination (our unpublished data). The Mus81–Eme1 heterodimer is required for HR repair at stalled or broken replication forks and is also critical during mitotic (13,24,25) and meiotic HR (15,26). *In vitro*, Mus81–Eme1 can cleave various substrates that mimic stalled replication forks and nicked and intact HJs (15,27,28). Mus81–Eme1 not only has a binding and cleavage preference for nicked HJs but also has a robust cleavage activity on intact HJs (29). *S. pombe* meiotic cells deleted for *mus81* accumulate single HJs, as shown by 2D gel analysis and electron microscopy (8). The accumulation of HJs in *mus81Δ* cells results in severe meiotic defects (15) and sensitivity to the topoisomerase I poison camptothecin (CPT (30)); these phenotypes can be partially suppressed by expression of the *Escherichia coli* HJ resolvase RusA. Therefore, RusA has been used extensively, and is widely accepted, to identify the structures accumulated in various DNA repair mutants (15,26,30–32).

As described above, the last decade has seen major advances in the identification of activities most proximally involved in the processing of joint molecules (JMs) formed during HR. However, currently, little is known about how JM processing enzymes are recruited to their substrates, and whether their activities are facilitated by additional chromatin-associated factors. Interestingly, in this regard, others and we have identified and characterized the Smc5–Smc6 holocomplex, which seems to play multiple roles in HR (33). The octameric Smc5–Smc6 complex is structurally related to the cohesin and condensin complexes but, uniquely, contains two subunits, Nse1 and Nse2, which exhibit E3 ligase activity for ubiquitin and SUMO (Small Ubiquitin-like Modifier), respectively (33,34). In addition to Smc5, Smc6, Nse1 and Nse2, the complex contains a melanoma antigen-domain protein Nse3, a kleisin-like protein Nse4, and two armadillo/Huntington, Elongation Factor 3, PR65A, TOR repeat proteins, Nse5 and Nse6. Notably, unlike in budding yeast (33), *nse5Δ* and *nse6Δ* mutants are viable and display indistinguishable sensitivities to all tested DNA-damaging agents (35). In addition, Nse5 and Nse6 form a stoichiometric heterodimer when purified from insect cells (35) or bacterial cells (our unpublished data), and furthermore, *nse5Δ nse6Δ* double mutants are no more sensitive to UV irradiation than either single mutant (35). Thus, Nse5 and Nse6 function as an obligate heterodimer.

Reflecting key HR roles of the complex, Smc5–Smc6 in budding yeast and human cells is loaded near an enzymatically induced DNA DSB and is important for HR-mediated repair of the break (36–38). In addition, *smc5–smc6* mutation causes hypersensitivity to ionizing radiation (IR)-induced DSBs, which is not additive when combined with a *rad51* deletion; *smc5–smc6* mutants, like *rad51Δ* mutants, fail to restore chromosome integrity following IR (35,39–43). Intriguingly, the Smc5–Smc6 complex has been implicated in the processing of HR intermediates or suppression of their formation or both (reviewed in (33,44)). For example, *smc5–smc6* hypomorphs, including *nse2* E3 SUMO ligase-deficient cells, accumulate Rad51-dependent HR intermediates following replication stress, indicating a concerted action of the entire complex in the productive completion of HR (35,45–54).

What is the physical nature of the recombination structures that form when Smc5–Smc6 function is compromised? In budding yeast, a heterogeneous group of hemicatenane and converged replication fork structures arise during replication stress in Smc5–Smc6-deficient mitotic cells (45,47,48,55). These DNA structures appear similar to those that accumulate in *sgs1Δ* mutant cells, and thus, it has been proposed that Sgs1 acts in concert with Smc5–Smc6 and sumoylation in the removal of such linkages during vegetative growth (45).

Here, we identify a critical role for fission yeast Nse5–Nse6 in chromosome disjunction during meiosis. We use both genetic and physical assays to determine the underlying cause of meiotic failure in *nse6Δ* cells, the stage at which Nse5–Nse6 function is required, and the DNA structure(s) that prevent(s) chromosome segregation at the first meiotic division (MI) in *nse6Δ* cells. Our analyses demonstrate that Nse5–Nse6 acts after programmed meiotic DSB formation to drive the timely resolution of JMs whose persistence in *nse6Δ* cells causes the profound MI defects. The JMs observed in *nse6Δ* cells resemble the HJs that accumulate in *mus81Δ* cells, providing the first direct evidence for a role of the Smc5–Smc6 complex in HJ resolution. Although Nse5–Nse6 and Mus81 have some distinct roles, both proteins are essential to avoid an accumulation of JMs that impede meiosis. Here, we define Nse5–Nse6 as a novel regulator

of nuclear division, which may act directly in the HJ resolution mechanism or by attracting the Smc5–Smc6 complex to its needed sites of action—mitotic or meiotic HJs.

MATERIALS AND METHODS

Standard *Schizosaccharomyces pombe* techniques

Standard fission yeast methods and media were used in these studies (56). CPT was obtained from Sigma-Aldrich (St. Louis, MO). Table 1 lists the *S. pombe* strains, and Table 2 lists the primers used.

Unless otherwise indicated, all NBY strains are *ura4-D18* and *leu1-32*. pREP1-RusA, pREP1-RusA-D70N and pREP1 were described in (15). pE119, containing *LEU2* and *GST*, was used as a control vector (57). The minichromosome assay using Ch^{16}*-MHH*, Ch^{16}*-MGH* and *pREP81X-HO:LEU2* has been described in (58). Mutations other than mating type and commonly used auxotrophies are described in previous studies: *mus81::kanMX6* (15), *nse6::kanMX6* (35), *prh1::hphMX6* (this study), *rad51::ura4*$^+$ (59), *dmc1::hphMX6* (this study), *rec12-152::LEU2* (60), *mbs1-24* and *mbs1-25* (61), *bub-1243, vtc4-1104* (9), *lacO::lys1 lacI-GFP::arg3*$^+$ (62) and *nse6::natMX6* (the *kanMX6* marker in strain NBY835 (35) was switched to *natMX6* as described in (64)). In Table 1 ':' indicates marked by the following gene, and '::' indicates that the preceding gene is replaced by the following marker.

Polymerase chain reaction (PCR) was used to create the *hphMX6* cassette flanked by genomic DNA, to enable integration into the middle of the 1.2 kb intergenic region between the *prh1* and *SPAC2G11.10c* loci. The *hphMX6* cassette from pCR2.1 *hphMX6* (63) was amplified in two steps, using a combination of the primers shown in Table 2, as described in (63,64). A stable transformant was obtained with the *hphMX6* cassette integrated between *prh1* and *SPAC2G11.10c* loci, approximately 70 kb to the right of the *mbs1* meiotic DSB hotspot on chromosome I (61,65).

PCR was used to create the *hphMX6* cassette flanked by genomic DNA, to replace the *dmc1* gene. The *hphMX6* cassette from pCR2.1 *hphMX6* (63,64) was amplified in two steps, using a combination of the primers shown in Table 2, as described in (63,64).

HO-induced DSB repair assays

Cells were cultured in repressive (+ thiamine; B1) medium (EMM2), and a sample was plated onto non-selective medium (EMM2) for the 0 h time point. Cells were then cultured in repressive or de-repressive (−thiamine) media for 48 h and plated onto non-selective media. Colonies were counted after 3 days growth at 30°C. Replica plating onto media that contained hygromycin (or kanamycin for the *rad51Δ* mutant), or lacked either adenine or histidine, allowed calculation of the frequency of marker loss. Data are means and standard error of the mean from three independent assays, as described in (58).

Meiotic crosses and recombination assays

Cells from equal volumes (10 µl) of each parental haploid culture were mixed, washed, resuspended in water and plated onto supplemented sporulation agar plates (66). After 2 days at 25°C, the cell–ascus mixture was observed by microscopy or processed further for viability assays. Meiotic 4′,6-diamidino-2-phenylindole (DAPI) staining was performed essentially as described in (15). Zygotic asci were fixed in methanol (−80°C) for 10 min and then washed three times with phosphate-buffered saline (1× PBS). The fixed asci were treated with Zymolyase 100T (0.1 mg/ml) for 10 min at 37°C. Asci were collected by centrifugation and resuspended in 0.1% Triton X-100 for 2 min at room temperature. Asci were then washed three times (in 1× PBS) and resuspended in a drop of 1× PBS containing 0.5 µg/ml DAPI. Asci were photographed using a Nikon Eclipse E800 microscope equipped with a Photometrics Quantix CCD camera. Images were acquired with IPlab Spectrum software (Signal Analytics Corporation).

For viability assays, the cell–ascus mixture was suspended in 1 ml of H_2O and treated with 2% glusulase overnight at room temperature. Addition of ethanol to 30% for 1 h killed remaining vegetative cells, essentially as described in (67). To assess spore viability, spores were counted using a hemocytometer, diluted and plated onto the appropriate media. Spore viability was scored following incubation for 5–6 days at 30°C. For meiotic recombination assays, an appropriate dilution of spores was plated onto non-selective (YES) media and replica plated to appropriate test media: EMM2 (66) ± adenine for *ade7-152*; ± leucine for *leu1-32*; ± lysine for *lys4-95-*; ± histidine for *his4-239*; ± uracil for *ura1-61* and YES ± hygromycin (100 µg/ml) for *hphMX6*.

Analysis of recombination intermediates

pat1-114 strains were thermally induced for meiosis, and DNA was extracted from cells embedded in agarose plugs (68). The DNA was digested with appropriate restriction enzymes and analyzed by gel electrophoresis and Southern blot hybridization (8,69) and quantification (9).

The sensitivity of DNA to S1 nuclease (Roche) and to RuvC (gift of Ken Marians, Memorial Sloan-Kettering Cancer Center) was assayed by digesting the DNA, in plugs, with *Pvu*II restriction enzyme, followed by washing twice with TE (Tris-EDTA; 10 mM Tris–HCl, pH 7.0, 1 mM ethylenediaminetetraacetic acid (EDTA) pH 8.0) and twice with nuclease S1 buffer (33 mM sodium acetate, 100 mM NaCl, 0.033 mM $ZnSO_4$, pH 4.5 at room temperature) or RuvC buffer (50 mM Tris–acetate pH 7.5, 10 mM $Mg(OAc)_2$, 1 mM DTT, 50 µg of BSA per ml); duration for each wash was 20 min at room temperature. The plugs were incubated in 100 µl of buffer with the indicated amount of S1 for 2 h at 4°C or RuvC for 4 h at 4°C, then for 1 h at 37°C (S1) or for 4 h at 55°C (RuvC) to facilitate branch migration of HJs embedded in agarose; the digestions were stopped by adding 2.5 µl of 500 mM EDTA pH 8.0 and placing the incubation tubes on ice for 10 min. 2D electrophoresis was performed, and

Table 1. *Schizosaccharomyces pombe* strains and primers

Strain No.	Genotype
NBY128	*h*$^+$ *mus81::kanMX6*
NBY185	*h*$^-$ *pat1-114*
NBY282	*h*$^+$ *rec12-152::LEU2*
NBY355A	*h*$^-$ *mus81::kanMX6* (*pREP1:LEU2*)
NBY355C	*h*$^+$ *mus81::kanMX6* (*pREP1:LEU2*)
NBY356A	*h*$^-$ *mus81::kanMX6* (*pREP1-NLS-RusA:LEU2*)
NBY356C	*h*$^+$ *mus81::kanMX6* (*pREP1-NLS-RusA:LEU2*)
NBY364	*h*$^-$ *mus81::kanMX6* (*pREP1-NLS-RusA-D70N:LEU2*)
NBY365	*h*$^+$ *mus81::kanMX6* (*pREP1-NLS-RusA-D70N:LEU2*)
NBY384	*h*$^-$ *ade7-152 ura4*$^+$ (*pREP1:LEU2*)
NBY420	*h*$^+$ *ura1-61*
NBY780	*h*$^+$
NBY781	*h*$^-$
NBY835	*h*$^+$ *nse6::kanMX6*
NBY855	*h*$^-$ *rad51::ura4*$^+$ *nse6::kanMX6*
NBY871	*h*$^-$ *nse6::kanMX6*
NBY883C	*h*$^+$ *rec12-152::LEU2 nse6::kanMX6*
NBY896	*h*$^+$ *nse5::ura4*$^+$
NBY897	*h*$^-$ *nse5::ura4*$^+$
NBY917	*h*$^+$ *nse6::kanMX6* (*pREP1-NLS-RusA-D70N:LEU2*)
NBY936	*h*$^-$ *nse6::kanMX6* (*pREP1-NLS-RusA-D70N:LEU2*)
NBY952	*h*$^-$ *rad51::ura4*$^+$
NBY963	*h*$^-$ *nse6::kanMX6 ade7-152 leu1*$^+$ *ura4*$^+$
NBY991	*h*$^-$ *Ch*^{16}*-MHH ade6-210* (*pREP81X-HO:LEU2*)
NBY1000	*h*$^-$ *nse6::kanMX6 Ch*^{16}*-MHH ade6-210* (*pREP81X-HO:LEU2*)
NBY1484	*h*$^+$ *nse6::kanMX6* (*pE119:LEU2*)
NBY1486	*h*$^-$ *nse6::kanMX6* (*pE119:LEU2*)
NBY1753	*h*$^-$ *rec12-152:LEU2*
NBY2027	*h*$^+$ *rad51::ura4*$^+$
NBY2051	*h*$^+$ *rad51::ura4*$^+$ *nse6::kanMX6 lacO::lys1 lacI-GFP::arg3*$^+$
NBY2482	*h*$^+$ (*pREP1:LEU2*)
NBY2551	*h*$^-$ *dmc1::hphMX6*
NBY2589	*h*$^-$ *dmc1::hphMX6 nse6::kanMX6*
NBY2590	*h*$^+$ *dmc1::hphMX6 nse6::kanMX6*
NBY2610	*h*$^+$ *dmc1::hphMX6*
NBY2620	*h*$^+$ *rad51::ura4*$^+$ *dmc1::hphMX6 nse6::kanMX6*
NBY2621	*h*$^-$ *rad51::ura4*$^+$ *dmc1::hphMX6 nse6::kanMX6*
NBY2622	*h*$^+$ *rad51::ura4*$^+$ *dmc1::hphMX6*
NBY2623	*h*$^-$ *rad51::ura4*$^+$ *dmc1::hphMX6*
NBY2654	*h*$^+$ (*pREP1-NLS-RusA:LEU2*)
NBY2660	*h*$^+$ *nse6::kanMX6* (*pREP1-NLS-RusA:LEU2*)
NBY2750	*h*$^-$ *nse6::kanMX6* (*pREP1-NLS-RusA:LEU2*)
NBY2893	*h*$^+$ *ura1-61 nse6::kanMX6*
NBY2938	*h*$^+$ *pat1-114 nse6::natMX6*
NBY2953	*h*$^-$ *ura4*$^+$ *LEU2 his4-239 lys4-95*
NBY2962	*h*$^-$ *ura4*$^+$ *LEU2 his4-239 lys4-95 nse6::kanMX6*
NBY3112	*h*$^-$ *ura4*$^+$ *prh1:hphMX6*
NBY3114	*h*$^-$ *ura4*$^+$ *nse6::kanMX6 prh1:hphMX6*
NBY3304	*h*$^-$ *nse6::natMX6 mus81::kanMX6*
NBY3311	*h*$^+$ *nse6::natMX6 mus81::kanMX6*
NBY4176	*h*$^+$ *nse6::natMX6 mus81::kanMX6* (*pREP1-NLS-RusA:LEU2*)
NBY4178	*h*$^+$ *nse6::natMX6 mus81::kanMX6* (*pREP1:LEU2*)
NBY4192	*h*$^+$ *nse5::ura4*$^+$ (*pREP1-NLS-RusA:LEU2*)
NBY4194	*h*$^+$ *nse5::ura4*$^+$ (*pREP1:LEU2*)
NBY4195	*h*$^-$ *nse5::ura4*$^+$ (*pREP1-NLS-RusA:LEU2*)
NBY4197	*h*$^-$ *nse5::ura4*$^+$ (*pREP1:LEU2*)
NBY4198	*h*$^-$ *nse6::natMX6 mus81::kanMX6* (*pREP1-NLS-RusA:LEU2*)
NBY4200	*h*$^-$ *nse6::natMX6 mus81::kanMX6* (*pREP1:LEU2*)
NBY4298	*h*$^-$ *rad51::hphMX6 Ch*^{16}*-MGH ade6-210* (*pREP81X-HO:LEU2*)
GP1456	*h*$^-$ *rec12-152::LEU2 ura4-294 ade6-52*
GP5082	*h*$^-$/*h*$^-$ *ade6-216/ade6-210 pat1-114/pat1-114 +/ura1-61 mbs1-24/mbs1-25 his4-239/+ +/lys4-95 mus81::kanMX6/mus81::kanMX6*
GP5086	*h*$^-$/*h*$^-$ *ade6-216/ade6-210 pat-114/pat-114 +/ura1-61 mbs1-24/mbs1-25*
GP6234	*h*$^-$/*h*$^-$ *ade6-216/ade6-210 pat1-114/pat1-114 lys3-37/+ +/ura1-61 mbs1-24/mbs1-25 nse6::kanMX6/nse6::kanMX6*
GP6656	*h*$^-$/*h*$^-$ *ade6-3049/ade6-3049 bub1-243(L)/+ +/vtc4-1104(R) pat1-114/pat1-114 lys3-37/+ +/ura1-61 mbs1-24/mbs1-25 his4-239/+ +/lys4-95*
GP6657	*h*$^-$/*h*$^-$ *ade6-3049/ade6-3049 bub1-243(L)/+ +/vtc4-1104(R) pat1-114/pat1-114 lys3-37/+ +/ura1-61 mbs1-24/mbs1-25 his4-239/+ +/lys4-95 mus81::kanMX6/mus81::kanMX6*
GP7765	*h*$^+$/*h*$^+$ *ade6-3049/ade6-3049 bub1-243(L)/+ +/vtc4-1104(R) pat1-114/pat1-114 lys3-37/+ +/ura1-61 mbs1-24/mbs1-25 his4-239/+ +/lys4-95 mus81::kanMX6/mus81::kanMX6 nse6::kanMX6/nse6::kanMX6*
GP7773	*h*$^-$ *ade6-3049 pat1-114 nse6::kanMX6 rec12-171::ura4*$^+$

Table 2. Primers used to integrate the *hphMX6* marker between *prh1* and *SPAC2G11.10c* (primers 1–4) and to replace the *dmc1* gene with the *hphMX6* marker (primers 5–8)

Primer 1	5′-AATTGAGCTCTATTTCTGAG-3′
Primer 2	5′-TTAATTAACCCGGGGATCCGCTTTCATTTCAGT ACTTCAATCC-3′
Primer 3	5′-GTTTAAACGAGCTCGAATTCCATGGAGGTA ATTATTGGTTG-3′
Primer 4	5′-CTTTCTGGGCTTTCCTCACA-3′
Primer 5	5′-GCGACGCGTTCATTGTTAC-3′
Primer 6	5′-TTAATTAACCCGGGATCCGTGCACTTTATTTTT ATATTGAAC-3′
Primer 7	5′-GTTTAAACGAGCTCGAATTCTTGATTTTCTACC TATTCCA-3′
Primer 8	5′-AGTTGCTTTTGGGGGTTTG-3′

recombination intermediates were detected at *mbs1* as described in (8).

RESULTS

Roles of Nse5–Nse6 in mitotic DNA double-strand break repair

The budding yeast and human Smc5–Smc6 complexes have been implicated in the efficient repair of an enzymatically induced DNA DSB (36–38). To determine whether the fission yeast Nse5–Nse6 functionally interdependent heteromeric complex (35) plays an analogous role, we tested the DSB repair capacity of *nse6Δ* cells using a derivative of the non-essential minichromosome Ch^{16}, which contains the *MATa* target site for the *S. cerevisiae* HOmothallic switching (HO) endonuclease (see schematic in Figure 1A, described in (58)). Given the relatively mild IR sensitivity of fission yeast *nse6Δ* cells versus the extreme sensitivity of *rad51Δ* cells (35), it was surprising that both *nse6Δ* and *rad51Δ* cells were highly defective in the HR-based repair of the HO-induced break. Unlike wild-type cells, which repaired the majority of the HO-induced DSBs by gene conversion, the *nse6Δ* and *rad51Δ* mutants instead lost nearly all of the HO cut

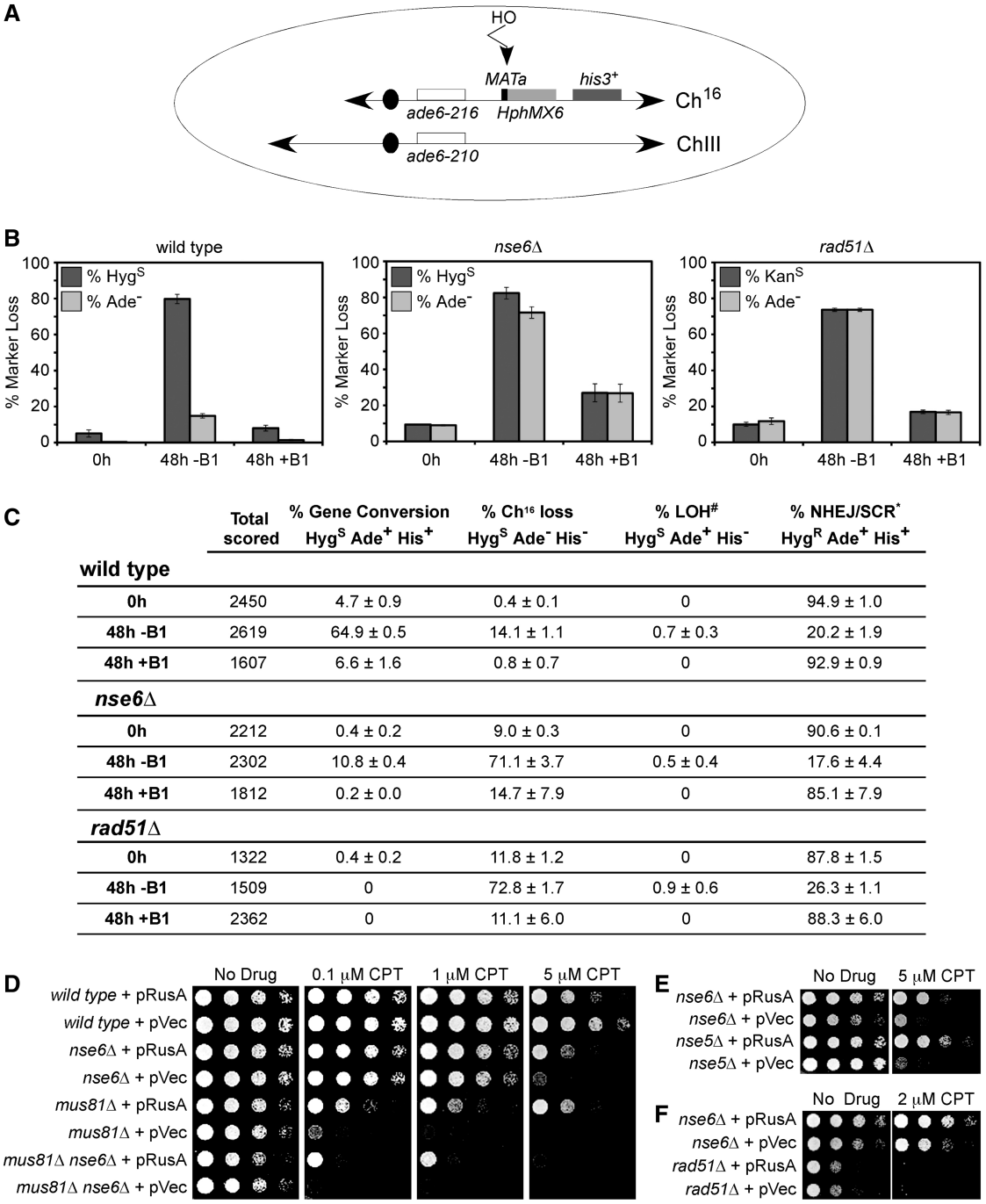

	Total scored	% Gene Conversion Hyg^S Ade^+ His^+	% Ch^{16} loss Hyg^S Ade^- His^-	% LOH# Hyg^S Ade^+ His^-	% NHEJ/SCR* Hyg^R Ade^+ His^+
wild type					
0h	2450	4.7 ± 0.9	0.4 ± 0.1	0	94.9 ± 1.0
48h -B1	2619	64.9 ± 0.5	14.1 ± 1.1	0.7 ± 0.3	20.2 ± 1.9
48h +B1	1607	6.6 ± 1.6	0.8 ± 0.7	0	92.9 ± 0.9
***nse6*Δ**					
0h	2212	0.4 ± 0.2	9.0 ± 0.3	0	90.6 ± 0.1
48h -B1	2302	10.8 ± 0.4	71.1 ± 3.7	0.5 ± 0.4	17.6 ± 4.4
48h +B1	1812	0.2 ± 0.0	14.7 ± 7.9	0	85.1 ± 7.9
***rad51*Δ**					
0h	1322	0.4 ± 0.2	11.8 ± 1.2	0	87.8 ± 1.5
48h -B1	1509	0	72.8 ± 1.7	0.9 ± 0.6	26.3 ± 1.1
48h +B1	2362	0	11.1 ± 6.0	0	88.3 ± 6.0

Figure 1. Mitotic roles for the Smc5–Smc6 complex. (**A**) Schematic of the HO-induced DSB minichromosome system. The minichromosome Ch^{16} and full-length Ch III with their centromeric regions (black ovals), histidine marker *his3*$^+$ (dark grey box) and complementing *ade6* heteroalleles (*ade6-216* and *ade6-210* (86); white boxes) are shown along with a *MATa* site for HO DSB formation (black rectangle) and the adjacent *hphMX6* (hygromycin)-resistance marker (light gray box) for wild-type and *nse6Δ* cells. As *rad51* was deleted using the hygromycin-resistance marker, a minichromosome bearing a *kan* (kanamycin)-resistance marker was used in this background. *MATa* is ∼25 kb from the *ade6* marker. Removal of thiamine (B1) derepresses the *HO* gene, whose product generates a DSB at the *MATa* target site (vertical arrowhead). HO-induced DSBs can result in (i) loss of Ch^{16} with diagnostic Ade^- and Hyg^S phenotype, (ii) repair of the DSB by interchromosomal gene conversion using Ch III as a template, resulting in the loss of *MATa* and *hphMX6* cassette and an Ade^+ and Hyg^S phenotype or (iii) maintenance of the initial Ade^+ Hyg^R phenotype, if the DSB is repaired by either non-homologous end-joining (NHEJ) or sister chromatid repair. The HO system can also assay levels of spontaneous minichromosome Ch^{16} loss, by scoring marker loss in the absence of HO induction (0 h, and 48 h culturing in thiamine). (**B**) and (**C**) Genetic analysis of site-specific DSB repair in wild-type (left panel), *nse6Δ* (middle panel) and *rad51Δ* (right panel) backgrounds. Percentage marker loss is given for cells grown in repressive (0 h and 48 h, +B1) or derepressive media (48 h, –B1). Data are means and standard errors from three independent experiments. #Loss of heterozygosity (LOH) can occur through various mechanisms, as described in (58). *Sister chromatid repair (SCR) also results in a Hyg^R Ade^+ phenotype. (**D**) RusA expression partially rescues the CPT sensitivity of *nse6Δ*, *mus81Δ* and *nse6Δ mus81Δ* mutants. (**E**) and (**F**) RusA expression partially rescues the CPT sensitivity of *nse5Δ* and *nse6Δ*, but does not rescue that of *rad51Δ* cells. (D–F) Five-fold serial dilutions of the indicated strains were plated onto medium that lacked thiamine to derepress plasmid-borne gene expression. Cells were either untreated or treated with the indicated concentrations of CPT and grown at 32°C for 3 days. pVec denotes an empty vector (87).

minichromosomes (Figure 1B and C (58,70)). This result indicates that in fission yeast, Smc5–Smc6, is required for the repair of enzymatically induced DSBs.

To test for an additional role of Nse6 in mitotic DNA break repair, we determined the sensitivity of *nse6Δ* mutants to CPT, which stabilizes topoisomerase I–DNA covalent complexes and can induce fork breakage during replication (30). The *nse6Δ* mutant was sensitive to CPT, although not as sensitive as *mus81Δ* or the *mus81Δ nse6Δ* double mutant [(71) and Figure 1D]. Although the expression of *E. coli* RusA HJ resolvase is mildly toxic to wild-type cells, as observed previously (72), the CPT sensitivities of both *nse6Δ* and *mus81Δ* cells were suppressed by RusA expression (Figure 1D). Notably, the *nse5Δ* mutant has a CPT sensitivity similar to that of *nse6Δ,* which is also rescued by RusA expression (Figure 1E). This result indicates a role for Nse5–Nse6, like Mus81, in HJ resolution. The *mus81Δ nse6Δ* double mutant was also suppressed by expression of RusA, although not as well as the single mutants, indicating that Nse5–Nse6 and Mus81 have distinct and overlapping roles. Although *nse6Δ* behaves like *rad51Δ* in the HO-induced DSB assay (Figure 1B and C (58)), the hypersensitivity of *rad51Δ* cells to CPT was not suppressed by RusA expression (Figure 1F).

Nse5–Nse6 executes an essential function during meiosis

Due to the similarity of the mitotic phenotypes of *nse5Δ, nse6Δ* and *mus81Δ* cells, we tested the role of Nse5–Nse6 in meiosis, an HJ-generating process that is heavily dependent on Mus81–Eme1 resolution activity (8,15,23). Wild-type meiosis produces asci with four haploid spores, with DNA present in each spore (Figure 2A). Asci from *nse5Δ* and *nse6Δ* mutant crosses were largely devoid of well-defined spores but infrequently contained one single large spore (Figure 2A), much like *mus81Δ* asci (15). This result shows that Nse5–Nse6 plays an important role in meiosis.

If Nse5–Nse6, like Mus81–Eme1, promotes JM resolution, then preventing the early stages of meiotic recombination should render Nse5–Nse6 unnecessary for meiotic nuclear division. For these tests, we first eliminated Rec12, which is essential for meiotic DSB formation and recombination (68). Asci from *rec12Δ* crosses were very heterogeneous: Some asci had four equal-sized spores like wild-type, some lacked spores or had only one like *nse6Δ* and many had two spores (dyads) like *rec12Δ* (Figure 2B; (7,15)). As anticipated, spore viability from homozygous *nse5Δ* or *nse6Δ* crosses was extremely low: Only ~0.5% of spores germinated and produced colonies, compared to ~80% for wild-type (Figure 2B (15)). Notably, both *rec12Δ* and *rec12Δ nse6Δ* crosses yielded similar spore viabilities of ~20%, and, furthermore, their ascus morphologies were indistinguishable (Figure 2B). The same was true for *rec12Δ* and *rec12Δ mus81Δ* crosses. The *rec12Δ nse6Δ* and *rec12Δ mus81Δ* double mutants had indistinguishable defects from those observed in a *rec12Δ* deletion, indicating that *rec12Δ* is epistatic to both *nse6Δ* and *mus81Δ* in meiosis.

The morphology of asci produced by crosses of *nse6Δ*, *mus81Δ* and *mus81Δ nse6Δ* double mutants were indistinguishable (Figure 2B). However, the viability of spores from *mus81Δ nse6Δ* crosses was ~8-fold lower than that of spores from crosses of the single mutants (Figure 2B). Deletion of *rec12* rescued the *mus81Δ nse6Δ* meiotic ascus phenotype, but only partially rescued the low spore viability phenotype, between 1 and 2% spore viability. Nevertheless, the spore viability in the *mus81Δ nse6Δ rec12Δ* triple mutant was about 1000-fold higher than that in the *mus81Δ nse6Δ* double mutant ($P < 0.0001$). These results indicate that Nse5–Nse6, like Mus81, acts in meiotic recombination after DSB formation by Rec12 (i.e. in the repair of DSBs).

Next, we exploited the aberrant ascus morphology of *nse6Δ* cells to determine whether Nse5–Nse6 acts before or after strand invasion promoted by the RecA homologs Rad51 and Dmc1 (4,5). Cells lacking Rad51 fail to repair many meiotic DSBs (73) but can produce asci containing four discrete, although mostly inviable, spores (15), presumably because there are no physical linkages, such as HJs, between the chromosomes to prevent their segregation (Figure 2C). Although not essential for meiotic progression and abundant formation of viable spores, Dmc1 is required for normal levels of meiotic recombination in most genetic intervals (4,9). In contrast to *rad51Δ* or *dmc1Δ* single mutants, four-spore asci were not observed in the *nse6Δ* single or *rad51Δ nse6Δ* or *dmc1Δ nse6Δ* double mutants (Figure 2B and C). However, the *dmc1Δ rad51Δ* double and *nse6Δ dmc1Δ rad51Δ* triple mutants produced similar asci that sometimes contained four spores, which are not observed for the *nse6Δ* single mutant (Figure 2B and C). Thus, suppression of the *nse6Δ* phenotype (to a level equivalent to that of the *dmc1Δ rad51Δ* double mutant) requires elimination of both strand-exchange proteins. These results indicate that Nse6 acts after strand exchange by Rad51 and Dmc1, perhaps during JM resolution.

Genetic and physical analyses of meiotic crossing over in *nse6Δ* cells

Next, we tested the impact of absence of Nse6 on meiotic recombination in three genomic intervals. In the large *ade7–leu1* interval, frequency of crossover among viable spores from a wild-type cross was 41.5%, not significantly different from the 40.8% in *nse6Δ* mutants (Figure 3A). In two shorter intervals, *lys4–his4* and *ura1–prh1* (which contains the *mbs1* DSB hotspot used in DNA analyses below (61)), frequencies of crossover were reduced by a factor of about 2 in *nse6Δ* mutants, relative to wild-type (Figure 3A), a statistically significant reduction ($P < 0.0001$). However, in contrast to the reductions by factors of 20–100 in *mus81Δ* cells (8,26), the meiotic crossover defects of *nse6Δ* cells are mild.

Through genetic methods, we can measure crossovers only in the ~0.5% of spores that are viable after *nse6Δ* meiosis; thus, our observed frequencies may overrepresent the frequencies in most of the cells. To circumvent this limitation, we physically measured the crossovers between two markers closely flanking the DSB hotspot

A

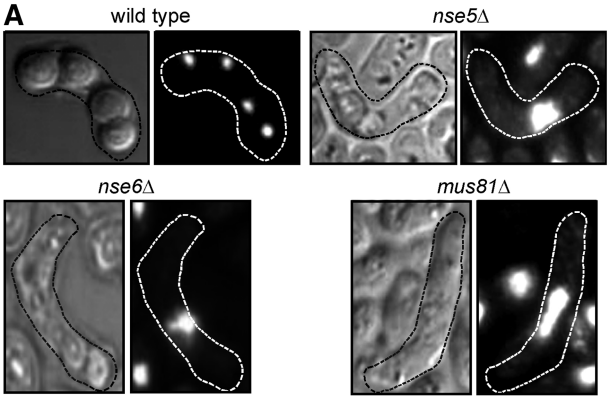

B

Genotype	% Ascus Phenotype					% Viability
						
wild type	85	7	4	0	4	80
nse5Δ	0	0	0	85	15	0.09
nse6Δ	0	1	0	90	9	0.33
rec12Δ	14	16	7	52	11	22.4
nse6Δ rec12Δ	15	11	8	58	8	19.2
mus81Δ	0	0	0	86	14	0.016
mus81Δ rec12Δ	17	14	4	51	14	21.7
mus81Δ nse6Δ	0	0	0	89	11	0.002
mus81Δ nse6Δ rec12Δ	14	10	0	60	16	1.5

C

Genotype	% Ascus Phenotype					% Viability
						
wild type	85	7	4	0	4	80
nse6Δ	0	1	0	90	9	0.33
dmc1Δ	75	3	2	19	1	27
nse6Δ dmc1Δ	0	0	0	95	5	0.28
rad51Δ	18	3	2	55	22	0.77
nse6Δ rad51Δ	0	0	0	92	8	0.35
rad51Δ dmc1Δ	10	6	5	52	27	0.3
nse6Δ rad51Δ dmc1Δ	13	3	1	64	19	0.4

Figure 2. The Smc5–Smc6 complex acts after DSB formation and strand invasion during meiotic recombination. (**A**) Cells lacking Nse6 or Nse5 form aberrant asci following meiosis. Mature asci (phase microscopy on the left or DAPI stained on the right) outlined with a dashed line, from genetic crosses of wild-type, *nse5Δ*, *nse6Δ* and *mus81Δ* cells. Two days after mating, wild-type asci show four spores of equal size, each containing DNA. *nse5Δ*, *nse6Δ* and *mus81Δ* mutants do not form well-defined spores, with progeny often having only one large spore. (**B**) The low spore viability of *nse6Δ*, *mus81Δ* and the *nse6Δ mus81Δ* double mutant is rescued by deleting *rec12*. The percentage of asci with either a wild-type appearance (four well-defined spores of equal size) or aberrant phenotypes including triads, dyads (typical for *rec12Δ*), or a single large spore, or four very small spores (as observed in *nse6Δ* cells) was determined. Spore viabilities were scored for crosses of the indicated genotypes. Data shown are the averages from three independent crosses, and around 100 asci were counted for each cross. (**C**) Nse6 acts after the Rad51 and Dmc1 strand-exchange proteins. The percentage of asci produced from a genetic cross of *rec12Δ*, *rad51Δ*, *dmc1Δ* and *mus81Δ* strains (either as single or double mutants) in the presence or absence of Nse6 is shown. Black areas indicate spores of various sizes and shapes.

mbs1 in the entire meiotic population, as previously analyzed in *mus81Δ* mutants (8). The crossover-specific product R2 (Figure 3B) was quantified in wild-type, *mus81Δ*, *nse6Δ* and *nse6Δ mus81Δ* strains at 7 h after induction of synchronous meiosis. Consistent with previous data (8), there was a severe defect, a reduction by a factor of 7, in crossover formation in *mus81Δ* and *nse6Δ mus81Δ* cells (Figure 3B). Importantly, in *nse6Δ* cells, crossover formation was reduced by a factor of about 2, as in the genetic assay for *ura1–mbs1–prh1* recombinants (Figure 3A), suggesting that Nse5–Nse6 promotes but is not absolutely essential for meiotic crossover formation (Figure 3B).

Recombination intermediates (DNA joint molecules) accumulate in *nse6Δ* mutants

The similarities of the vegetative and meiotic phenotypes of *mus81Δ* and *nse6Δ* led us to investigate whether DNA JMs accumulate during meiosis in *nse6Δ*, as they do in *mus81Δ* (8). Synchronous meiosis was induced in *pat1-114 nse6Δ* and *nse6Δ mus81Δ* diploids, and the formation of branched DNA structures, indicative of both replication and recombination intermediates, was analyzed via 2D gel electrophoresis as previously performed for *mus81Δ* (8). Branched DNA structures produced during replication were visible at 2.5 h and decreased toward 3 h (Figure 4A and B), the time at which DNA content shifts from 2n to 4n as measured by flow cytometry ((8); our unpublished data). After replication was complete and DSB formation had begun (Figure 4C), the amount of X-shaped DNA increased again at 4 h, persisted at 4.5 h and disappeared after 5 h in the wild-type strain (Figure 4A and B), as expected for the formation and resolution of HJs. In the *nse6Δ* strain, the recombination intermediates were formed with the same timing as in wild-type, but they did not disappear; the same was true for *mus81Δ* and *nse6Δ mus81Δ* mutants, although the double mutant showed a slight delay in JM formation (Figure 4A and B; (8)). As expected, early but not late appearing JMs were detected in an *nse6Δ rec12Δ* haploid double mutant (haploid and diploid analyses are indistinguishable (74) and our unpublished data). This result indicates that, as in *mus81Δ* mutants (8), the early arising JMs are replication derived, and the late arising JMs are recombination intermediates and are consistent with the meiotic phenotype of *nse6Δ* depending on DSB formation by Rec12 (Figure 2B). Thus, both *nse6Δ* and *mus81Δ* mutants accumulate recombination intermediates with a similar timing during meiosis.

Next, we determined whether the JMs that accumulate in the *nse6Δ* mutant specifically form between sister

A

wild type				CO frequency	
Interval	**Ch.**	**kb**	**# Scored**	**%**	**cM**
ade7 - leu1	II	817	2472	41.5	86
lys4 - his4	II	76	1726	6.7	7.2
ura1 - prh1	I	89	1640	9.5	10.5

nse6Δ				CO frequency	
Interval	**Ch.**	**kb**	**# Scored**	**%**	**cM**
ade7 - leu1	II	817	874	40.8	85
lys4 - his4	II	76	1821	2.5	2.6
ura1 - prh1	I	89	3403	6.2	6.5

B

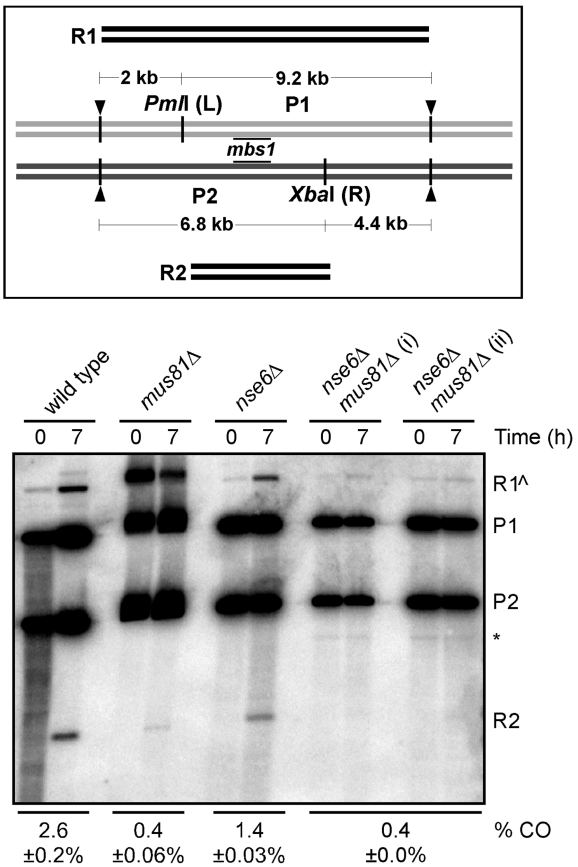

Figure 3. Effect of *nse6Δ* mutation on the frequency of meiotic crossovers. (**A**) Crossover (CO) frequencies in three intervals in the wild-type and *nse6Δ* backgrounds. The percent of recombinant spore colonies was converted into genetic distance in centimorgans with Haldane's equation. The number of colonies analyzed is the total from at least three independent experiments. (**B**) Amount of crossover DNA generated at the *mbs1* hotspot (8). Diploid *pat1-114* wild-type (GP6656), *mus81Δ* (GP6657), *nse6Δ* (GP6234) and *nse6Δ mus81Δ* (GP7765) strains with heterozygous restriction sites *Pml*I (L) and *Xba*I (R) flanking *mbs1* were assayed. Digestion with these enzymes and *Pvu*II (black arrowheads), which cuts outside L and R, gives two parental DNA fragments [9.2 kb (P1) or 6.8 kb (P2)] and two recombinant DNA fragments [11.2 kb (R1) or 4.8 kb (R2)] detected by the Southern blot hybridized probe (black lines at *mbs1*). The crossover DNA was measured at 7 h, after JM resolution in wild-type strains (Figure 4A, top); a pre-meiotic 0 h is shown as a control. Because R1 can also arise from incomplete digestion (R1^) at either L or R, the frequency of crossover DNA (% CO) was calculated as two times the amount of R2 DNA divided by the amount of total DNA. DNA from two independent inductions of strain GP7765 (*nse6Δ mus81Δ*) are shown. The means of two to three experiments (some from additional unpublished experiments) with the range or standard error of the mean are given. The asterisk indicates a non-specific cross-hybridization band.

chromatids or between homologs, and whether they are single HJs, as they are in a *mus81Δ* mutant (8), and not double HJs, a plausible alternative. A strain with heterozygous restriction site mutations that flank the DSB hotspot *mbs1* was used to assay the relative interhomolog (IH) and intersister (IS) HJs formed during DSB repair. As was the case in the *mus81Δ* strain (8,9), IS HJs outnumbered IH HJs by ~3.5:1 (Figure 5A). To distinguish single versus double HJs, the DNA in the agarose gel after the first dimension of electrophoresis was heated to 65°C to promote branch migration. The unequal length arms of homologous DNA in single HJs, which have two recombinant DNA strands, prevent the junction from migrating past the ends of the arms; the absence of recombinant DNA strands in double HJs and the equal length homologous arms of IS HJs allow their junctions to readily migrate off the end (8). When the DNA was heated, the IS HJs readily branch migrated and disassociated into the linear forms, whereas the IH HJs were resistant and remained intact (Figure 5B). This stability indicates that the IH-branched DNA structures are single HJs. This is the same behavior observed previously for branched DNA that accumulates in the *mus81Δ* mutant (8). These physical analyses further support a role for Nse6 in the resolution of DNA JMs during meiosis.

The X-shaped DNA structures seen in the 2D gel assays could be either HJs or a related four-stranded DNA structure, a hemicatenane, with two single DNA strands, or two pairs of strands, interwound. We first tested the sensitivity of these structures to the *E. coli* HJ resolvase RuvC (75). The JMs of the *nse6Δ* and *mus81Δ* strains were similarly sensitive to RuvC (Figure 6A and B), indicating that at least some of the X-shaped structures formed in both *mus81Δ* and *nse6Δ* strains are the same and are HJs. However, the JMs of the *nse6Δ mus81Δ* strain were largely resistant, suggesting that these X-shaped structures are not HJs but might be related structures such as hemicatenanes.

Although structurally similar to HJs, hemicatenanes have exposed ss DNA that would be susceptible to S1, a nuclease more active on ss DNA than on double-stranded DNA (76). To test this possibility, meiotic DNA prepared at 4.5 or 5 h after induction of *mus81Δ* or *nse6Δ* strains was treated with S1 before 2D gel electrophoresis. The accumulated branched DNA structures from the *mus81Δ* strain were insensitive to S1 treatment, but those from the *nse6Δ* and *nse6Δ mus81Δ* strains were partially sensitive

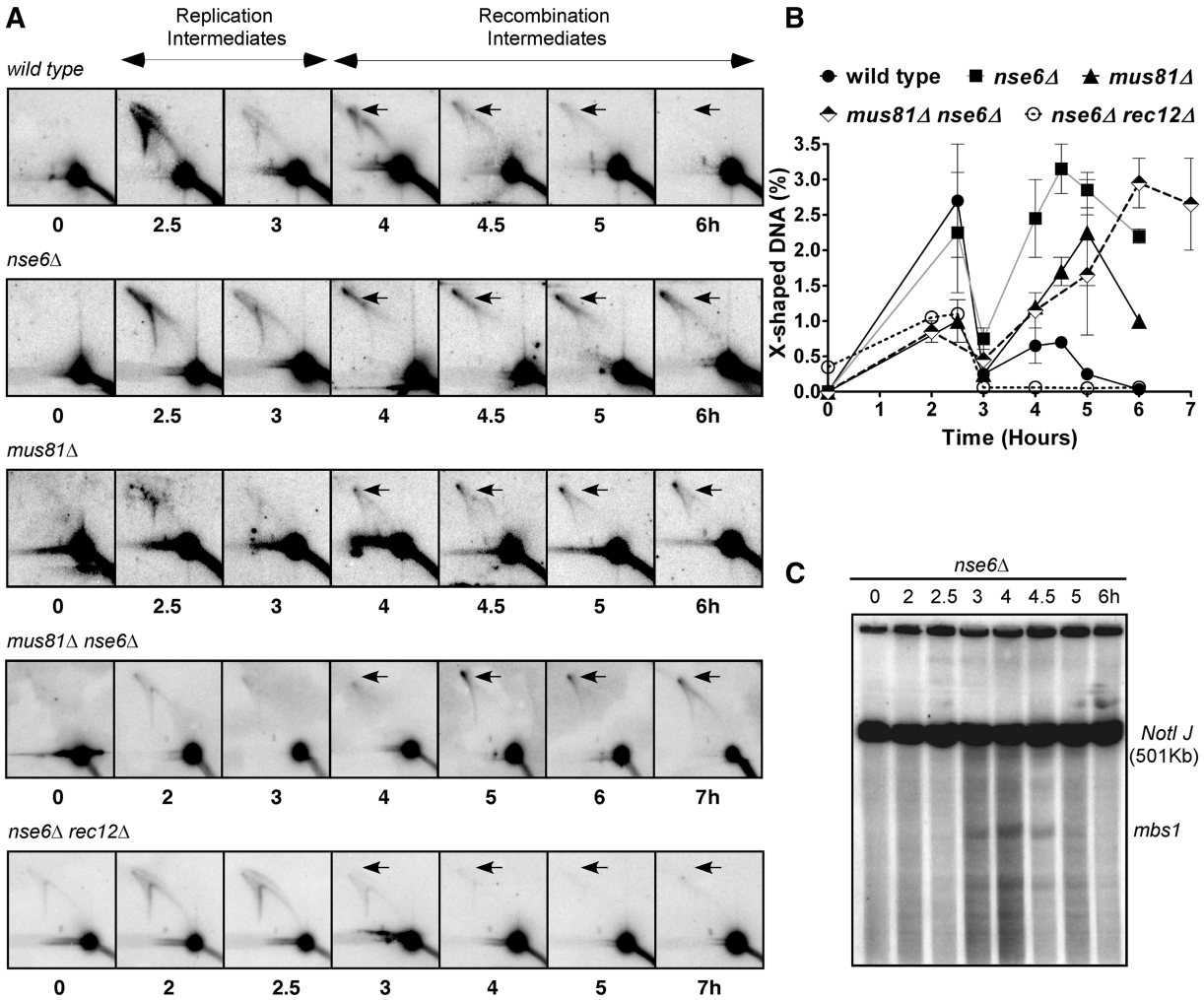

Figure 4. Joint molecules accumulate during meiosis in the *nse6Δ* mutant. (**A**) Diploid *pat1-114* wild-type (GP6656), *nse6Δ* (GP6234), *mus81Δ* (GP6657) and *nse6Δ mus81Δ (*GP7765) and haploid *pat1-114 nse6Δ rec12Δ* (GP7773) strains were induced for meiosis. DNA was extracted at the time indicated and digested with *Pvu*II to generate 11.2 kb DNA fragments containing *mbs1* (Figure 3B). Branched DNA molecules were assayed by two-dimensional gel electrophoresis (8,88) in which the first dimension slowly separates DNA primarily by mass and the second dimension primarily by shape, as branched structures have less mobility than linear DNA, and subsequent Southern blot hybridization. DNA from 2.5–3 h shows branched DNA structures arising from replication, while at 4 h, the structures are primarily recombination intermediates (8). Note that X-shaped DNA (arrows) forms in the wild-type at 4 h and disappears by 6 h, as expected for HJs that form and are resolved during the repair of DSBs, but form and persist in *nse6Δ, mus81Δ* and *nse6Δ mus81Δ* mutants. (**B**) Quantification of the X-shaped DNA observed in (A). Each datum is the mean of two independent experiments, with the error bars indicating the range. (**C**) Meiotic DSBs arise and disappear with wild-type timing in a diploid *nse6Δ* strain GP6234. DNA prepared at the indicated time after induction of meiosis was digested with *Not*I, separated by pulsed-field gel electrophoresis and analyzed by Southern blot hybridization with a probe specific to the left end of the 501 kb *Not*I fragment J, which contains *mbs1* near its middle. Note that DSBs appear after replication at 3 h, reach a maximum at 4 h and are mostly repaired by 5 h, consistent with previous results from wild-type and *mus81Δ* strains (8,9,68,69) and with the timing of HJ formation observed in (A).

(Figure 6A and B). We propose that both HJs and an S1-sensitive form of DNA, such as hemicatenanes, accumulate in *nse6Δ* mutants but only HJs accumulate in *mus81Δ* mutants during meiosis (Figure 6A and B).

Suppression of *nse5Δ* and *nse6Δ* meiotic defects by bacterial resolvase RusA

Our biochemical analyses provide evidence that *nse6Δ* mutants accumulate meiotic HJs, as observed in *mus81Δ* mutants (8,15). For *in vivo* validation of this conclusion, we used the RusA resolvase to probe the nature of the meiotic impediment in *nse5Δ* and *nse6Δ* cells. Our laboratories and others have shown that heterologous expression of *E. coli* RusA reduces the level of HJs that accumulate either on treatment with various DNA damaging agents or during meiosis in various DNA repair mutants (15,26,30–32). We expressed RusA and its catalytically inactive mutant, D70N, in *nse6Δ* cells and analyzed both spore formation and viability. Strikingly, RusA expression significantly rescued the meiotic defects of *nse6Δ* cells, yielding asci that often contained a wild-type complement of four spores (Figure 6C). This rescue required RusA endonuclease activity, as the RusA-D70N catalytically inactive mutant provided no benefits (Figure 6C). The spore viability was increased

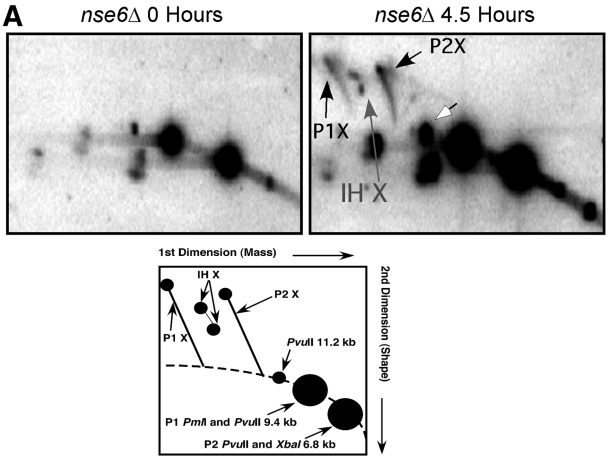

B % JM relative to linear DNA (± SEM)

Strain	IS1 HJ	IS2 HJ	IH HJ	Ratio [IS1+IS2] :IH
wild type	0.26 ± 0.06	0.27 ± 0.04	0.14 ± 0.01	3.8:1 (n=5)
mus81Δ	1.09 ± 0.18	0.83 ± 0.15	0.52 ± 0.13	3.7:1 (n=5)
nse6Δ	1.1 ± 0.1	0.9 ± 0.1	0.6 ± 0.07	3.3:1 (n=5)

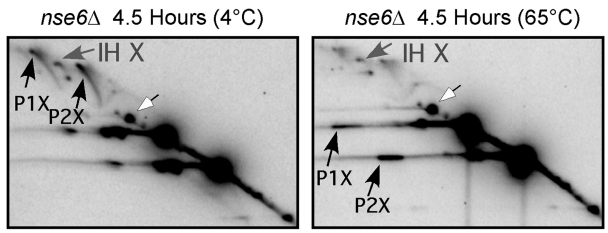

Figure 5. IS and IH JMs accumulate in *nse6Δ* cells. (**A**) DNA prepared before (0 h) or 4.5 h after meiotic induction was digested with *Pvu*II, *Pml*I and *Xba*I and separated by 2D-gel electrophoresis and Southern blot hybridized to assay for IS and IH JMs at *mbs1* (8). DNA fragments with different masses are created with heterozygous restriction site mutations (depicted in cartoon). Parental fragments of 9.2 or 6.8 kb give rise to IS JMs (black arrows) that contain 18.4 or 13.6 kb of DNA, respectively. IH JMs (gray arrows) have an intermediate mass of 16 kb. Both IS and IH JMs accumulate, and the IS JMs outnumber the IH JMs 3.3 to 1, consistent with the 3.8:1 ratio previously observed in a *mus81Δ* mutant (8). The mean ± standard error of the mean of five experiments is indicated. (**B**) Branch migration of the JMs from the *nse6Δ* mutant, like those from *mus81Δ*, suggests single, not double, HJs. DNA prepared at 4.5 h after meiotic induction of an *nse6Δ* strain (GP6234) was digested as in (A). After the first dimension of electrophoresis, the DNA, in agarose, was incubated at either 4 or 65°C for 6 h, and the DNA was then subjected to the second dimension of electrophoresis. As expected, no detectable branch migration of JMs occurred at 4°C, but at 65°C, both IS JM species almost completely dissociated into parental length DNAs (black arrows). The IH JMs (gray arrows), however, remained intact, which is the characteristic of single HJs, as previously observed in a *mus81Δ* mutant (8). White arrows in (A) and (B) indicate partial digestion by either *Pml*I or *Xba*I, which results in the full-length 11.2 kb *Pvu*II restriction fragment (the same as R1 in Figure 3B).

more than 20-fold when RusA was expressed in *nse6Δ* cells compared to an empty vector control (Figure 6D). Spore viability was also increased in *nse5Δ* cells (Figure 6D). Likewise, although more dramatic due to their initial lower viability, *mus81Δ* spore viability was increased more than 800-fold by RusA expression. Interestingly, spore viability was around 1.5% in *nse5Δ* and 3% in *nse6Δ* mutants expressing RusA, which was significantly lower ($P < 0.005$) than in *mus81Δ*-expressing RusA (7%; Figure 6D). This result is consistent with the accumulation of both HJs and an S1-sensitive form of DNA, such as hemicatenanes, in *nse5Δ* and *nse6Δ* meiosis, but only HJs in *mus81Δ* meiosis (Figure 6A and B). RusA expression did not so strongly improve the ascus morphology or spore viability in the *nse6Δ mus81Δ* double mutant (Figure 6C and D), which is consistent with the RuvC insensitivity of DNA isolated from these cells (Figure 6A and B). Overall, the remarkably similar suppression of both the ascus morphology and spore viability defects in *nse5Δ* or *nse6Δ* and *mus81Δ* by RusA endonuclease suggests that Nse5–Nse6 plays a role in facilitating the HJ resolvase activity of Mus81–Eme1.

DISCUSSION

Failure of the HR pathways underlies many human diseases including cancer and can cause birth defects through aberrant meiotic chromosome segregation. Here, we have identified a novel function for Nse5–Nse6 of the Smc5–Smc6 complex in processing mitotic and meiotic HR intermediates. Genetic and physical analyses indicate that *nse6Δ* mutants accumulate JMs resembling the HJs that accumulate in *mus81Δ* during meiosis. Thus, to our knowledge, Nse5–Nse6 is only the second factor in fission yeast required for the endonucleolytic processing of HJs, besides Mus81–Eme1, which has the catalytically active site for HJ resolution.

The key data supporting a function for Nse5–Nse6 in the resolution of JMs are as follows: (i) like *mus81Δ* mutants (15), *nse6Δ* mutants form few viable spores (Figure 2), due to the failure of chromosome segregation; (ii) like *mus81Δ* (15), *rec12Δ* is epistatic to *nse6Δ* in meiosis, demonstrating that Nse5–Nse6 acts after DSB formation (Figure 2); (iii) the double *nse6Δ mus81Δ* mutant also forms few viable spores and is suppressed, at least partially, by *rec12Δ*, indicating that Mus81 and Nse6 act in the same or closely related steps of meiosis (Figure 2); (iv) the *rad51Δ dmc1Δ* combination is epistatic to *nse6Δ*, demonstrating that Nse5–Nse6 acts after the formation of JMs (Figure 2); (v) JMs accumulate in meiotic *nse6Δ* and *nse6Δ mus81Δ* cells, and these JMs are temporally, genetically and electrophoretically indistinguishable from the HJs that accumulate in *mus81Δ* cells (Figures 4 and 5, (8)); (vi) at least some of these JMs are sensitive to *E. coli* RuvC HJ resolvase (Figure 6) and to RusA HJ resolvase, because, as for *mus81Δ* cells (15), expression of RusA partially rescues the meiotic defects of *nse6Δ* cells (Figure 6C and D) and (vii) crossovers are modestly reduced in *nse6Δ* cells, indicating that Nse5–Nse6 is important but not absolutely essential for HJ resolution, which requires Mus81–Eme1 (Figure 3).

In addition to HJ resolution, Nse5–Nse6 appears to have a second role because (i) the double *nse6Δ mus81Δ* mutant grows more slowly and is more CPT sensitive than either single mutant (Figure 1D); (ii) the double mutant is

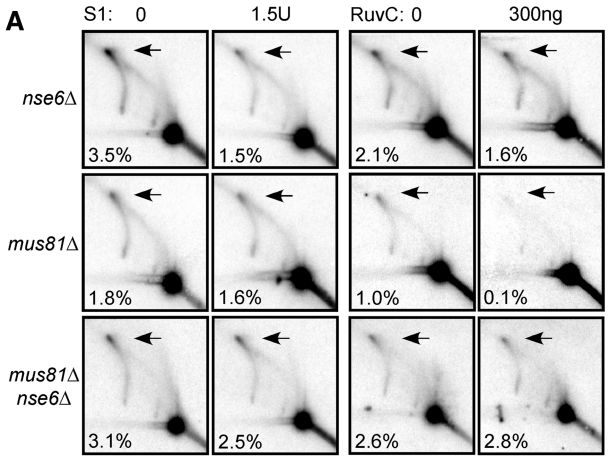

B

	*nse6*Δ		*mus81*Δ		*mus81*Δ *nse6*Δ	
S1	-	+	-	+	-	+
	2.8 ± 0.3	1.7 ± 0.2	1.7 ± 0.2	1.6 ± 0.3	3.0 ± 0.6	2.2 ± 0.2
RuvC	-	+	-	+	-	+
	2.1 ± 0.4	1.0 ± 0.4	1.9 ± 0.3	0.6 ± 0.3	2.2 ± 0.4	2.0 ± 0.7

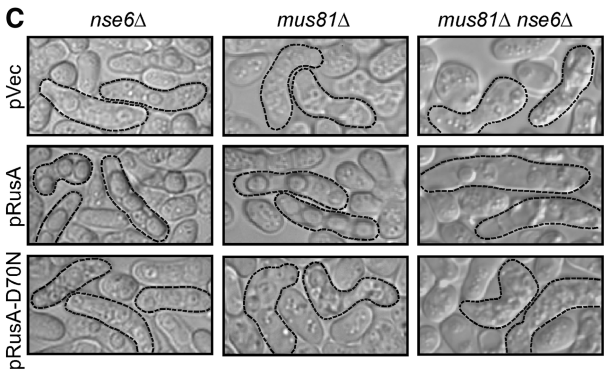

D

		+B1		-B1		
	Strain	**% Spore Viability**	**SEM**	**% Spore Viability**	**SEM**	**(n=)**
*nse6*Δ	pVec	0.11	0.017	0.09	0.014	7
	pRusA	0.13	0.022	3.1	0.41	17
	pRusA-D70N	0.04	0.008	0.10	0.021	6
*mus81*Δ	pVec	0.002	0.00073	0.005	0.0014	4
	pRusA	0.17	0.045	7.0	0.98	4
	pRusA-D70N	0.003	0.00042	$<1.2 \times 10^{-5}$	N/A	4
*mus81*Δ *nse6*Δ	pVec	4.5×10^{-5}	4.5×10^{-5}	0.00012	7.9×10^{-5}	4
	pRusA	0.00013	6.9×10^{-5}	0.00092	0.00031	4
*nse5*Δ	pVec	0.041	0.0089	0.021	0.0048	3
	pRusA	0.034	0.029	1.5	0.13	3

Figure 6. *nse6Δ* Mutants fail in meiosis because of DNA joint molecule accumulation. (**A**) DNA prepared at 4.5 or 5 h (*nse6Δ* and *mus81Δ*) or 6 h (*nse6Δ mus81Δ*) after meiotic induction was digested with *Pvu*II and treated with the indicated amounts of either the ss DNA-specific S1 nuclease or the purified RuvC and assayed by two-dimensional gel electrophoresis and Southern blot hybridization using the probe shown in Figure 3B. The percentage given is the amount of JMs, indicated by arrows, divided by the amount of total DNA. All

not quite as well suppressed to CPT resistance by expression of RusA as the single mutants (Figure 1D); (iii) unlike *mus81Δ*, *nse6Δ* is defective for mitotic DSB repair, as is *rad51Δ* (Figure 1); (iv) crossovers are formed, although at reduced level compared to wild-type, in *nse6Δ* but not in *mus81Δ* or *nse6Δ mus81Δ* mutants (Figure 3) and (v) the JMs that accumulate in *nse6Δ* and *nse6Δ mus81Δ* meiotic cells are at least partially sensitive to S1 nuclease, whereas those that accumulate in *mus81Δ* meiotic cells are not (Figure 6A and B), suggesting that Mus81–Eme1 and Nse6 have distinct, and overlapping, roles.

To reconcile these observations, we propose that in meiotic cells Nse5–Nse6 stimulates the resolution of HJs by Mus81–Eme1 and the resolution of other structures, such as hemicatenanes, which may arise during mitotic growth or during meiosis in the absence of Mus81–Eme1. These structures may arise during mitotic replication, as suggested by others (45,77), thereby partially accounting for the mitotic phenotypes of *nse6Δ* mutants. The structure of the JMs that accumulate in *nse6Δ* and *nse6Δ mus81Δ* mutants is not entirely clear, although those that accumulate in *mus81Δ* mutants are clearly single HJs (8). The JMs that accumulate in *nse6Δ* mutants are sensitive to both S1 nuclease and RuvC HJ resolvase, whereas those that accumulate in *mus81Δ* mutants are sensitive to RuvC and those in *nse6Δ mus81Δ* mutants are sensitive to S1 nuclease (Figure 6A and B). The stimulation of Mus81 HJ resolvase activity by the Nse5–Nse6 complex may be direct or indirect.

We propose that in *nse6Δ* mutants, Mus81–Eme1 slowly resolves HJs while some are converted into another structure and that in *nse6Δ mus81Δ* mutants, most or all of the HJs are converted into this structure. This proposal is consistent with the slight reduction in meiotic crossover frequency, among the few viable spores that arise, in *nse6Δ* mutants but strong reduction in *mus81Δ* mutants (Figure 3A (8,23,26)); with the slight reduction in total crossover DNA in *nse6Δ* mutants but strong reduction in *mus81Δ* and *nse6Δ mus81Δ* mutants (Figure 3B (8)); and with the suppression of *nse6Δ*, but not *nse6Δ mus81Δ*, by expression of the RusA HJ resolvase (Figure 6C and D).

The resistance to branch migration of the IH JMs in *nse6Δ* mutants suggests that these JMs, between heterozygous restriction sites, are single HJs with recombinant length strands (Figure 5B). This is because either double HJs, which have parental length strands, or hemicatenanes

Figure 6. Continued
experiments shown were performed concurrently. **(B)** The mean of two to five experiments performed as in (A), with either the range or standard error of the mean indicated. **(C)** *nse6Δ*, *mus81Δ* or *mus81Δ nse6Δ* mutants carrying an empty vector (pVec), pRusA or catalytically inactive pRusA-D70N were mated and sporulated, and the resultant asci photographed. Mature asci, outlined with a dashed line, arose from a meiotic cross of the indicated cells in medium lacking thiamine (B1) to allow vector-borne gene expression. **(D)** Spore viabilities were determined for *nse5Δ*, *nse6Δ*, *mus81Δ* or *mus81Δ nse6Δ* mutants bearing the indicated vectors and grown in media that either repressed (+B1) or derepressed (-B1) plasmid-borne gene expression. Spore viability data are the means from 3–17 independent experiments.

with either recombinant or parental length strands should dissociate into separate duplexes on heating (e.g. (8,76,78)). IS JMs would dissociate in any case, as observed. IH and IS JMs may differ in structure, but their low level has precluded our determining their sensitivity to S1 nuclease and RuvC. Although the S1 nuclease sensitivity is consistent with some JMs being hemicatenanes, to our knowledge, this structure has not been clearly demonstrated to arise in cells, for example by electron microscopy or comparison with synthetic DNA molecules. Further investigation is required to establish the structure of the population of non-HJ containing JMs in the absence of Nse6.

As Nse5–Nse6 acts as part of the Smc5–Smc6 complex, which has multiple roles in chromosome metabolism (44), it is no surprise that Nse5–Nse6 has multiple roles. One tempting hypothesis is that during meiosis, the primary role of Nse5–Nse6 is to stimulate the Mus81–Eme1 HJ resolvase and that during mitotic growth it plays both this and a second role. During both stages of the life cycle, expression of RusA suppresses at least partially the *nse6Δ* phenotype (Figures 1D and 6C and D), indicating that HJ resolution is stimulated by Nse5–Nse6 in both stages. The second role of Nse5–Nse6 might be to regulate any of the multiple functions of the Smc5–Smc6 complex (44). Further investigation is required to elucidate this function, but the requirement for Rad51 and Nse6 but not Mus81–Eme1 in mitotic DSB repair (Figure 1) suggests that Nse5–Nse6 is also important for the synapsis phase of mitotic DSB repair.

Although the Nse1 and Nse2 E3 ligase activities, like Nse5–Nse6, facilitate mitotic DNA repair (79–81), neither of these E3 ligases is required for meiotic nuclear division and recombination [(82) our unpublished data]. Thus, although the mitotic functions of Nse1, Nse2 and Nse5–Nse6 have not been dissected, in meiosis, Nse5–Nse6 acts independently of posttranslational modifications catalyzed by Nse1 and Nse2. Nevertheless, on the basis of our previous analyses showing that hypomorphic mutants of the essential Smc5–Smc6 subunits exhibit catastrophic meioses (83), we propose that Nse5–Nse6 acts in conjunction with the Smc5–Smc6 holocomplex to execute its meiotic HR role.

Budding yeast *smc5–smc6* mutations also disrupt meiotic nuclear division (84), but the underlying defects appear strikingly different from those of *nse6Δ* fission yeast. Key differences are that a *spo11* (*rec12* homolog) mutation is not epistatic to an *smc5–smc6* mutation, and crossovers are not affected in *smc6* temperature-sensitive (Ts) mutant cells (84). Thus, the authors concluded that the crucial role of Smc5–Smc6 is executed during premeiotic S phase in budding yeast and not after the initiation of meiotic recombination. It is unclear whether this reflects real differences in the functions of Smc5–Smc6 between species or if the unavoidable disruption of both the essential and repair roles in *smc6* (Ts) budding yeast masks functions analogous to those of fission yeast Nse5–Nse6.

HJ resolution must be carefully controlled, both during mitotic growth and in meiosis. When a DNA strand lesion blocks mitotic replication, the fork can regress and form a structure whose center is identical to that of an HJ. Were it resolved by Mus81–Eme1, a DSB would be formed and require further processing to allow completion of replication. Alternatively, the regressed fork can migrate back to the original position and allow immediate continuation of replication. Thus, Mus81–Eme1 may be kept inactive during this time. If strand exchange between sisters or homologs forms an HJ that is present at the time of mitosis, HJ resolution would appear to be the most expedient means to allow chromosome segregation, and Mus81–Eme1 may be activated at this time [e.g. (19)]. Similarly, during meiosis, many dozens of HJs must arise to account for the ~45 crossovers in a fission yeast cell (85), and Mus81–Eme1 is clearly highly active in meiotic cells. We surmise that Nse5–Nse6, likely as part of the Smc5–Smc6 complex, regulates directly or indirectly the activity of Mus81–Eme1 allowing it to function at the proper time and place to maintain chromosome integrity and cell viability.

ACKNOWLEDGEMENTS

The authors thank Ken Marians for a generous supply of RuvC protein, Tim Humphrey for his kind gift of the minichromosome assay strain, Sue Amundsen for helpful comments on the article and Jay Patel for media preparation.

FUNDING

Scholar Award from the Leukemia and Lymphoma Society (to M.N.B.); National Institutes of Health (NIH) of the United States of America [GM068608 and GM081840 to M.N.B. and GM032194 to G.R.S.]. Funding for open access charge: NIH, United States.

Conflict of interest statement. None declared.

REFERENCES

1. McGlynn,P. and Lloyd,R.G. (2002) Recombinational repair and restart of damaged replication forks. *Nat. Rev. Mol. Cell. Biol.*, **3**, 859–870.
2. Mimitou,E.P. and Symington,L.S. (2011) DNA end resection—unraveling the tail. *DNA Repair*, **10**, 344–348.
3. Bishop,D.K., Park,D., Xu,L. and Kleckner,N. (1992) DMC1: a meiosis-specific yeast homolog of E. *coli* recA required for recombination, synaptonemal complex formation, and cell cycle progression. *Cell*, **69**, 439–456.
4. Fukushima,K., Tanaka,Y., Nabeshima,K., Yoneki,T., Tougan,T., Tanaka,S. and Nojima,H. (2000) Dmc1 of *Schizosaccharomyces pombe* plays a role in meiotic recombination. *Nucleic Acids Res.*, **28**, 2709–2716.
5. Haruta,N., Kurokawa,Y., Murayama,Y., Akamatsu,Y., Unzai,S., Tsutsui,Y. and Iwasaki,H. (2006) The Swi5-Sfr1 complex stimulates Rhp51/Rad51- and Dmc1-mediated DNA strand exchange in vitro. *Nat. Struct. Mol. Biol.*, **13**, 823–830.
6. Keeney,S., Giroux,C.N. and Kleckner,N. (1997) Meiosis-specific DNA double-strand breaks are catalyzed by Spo11, a member of a widely conserved protein family. *Cell*, **88**, 375–384.
7. Davis,L. and Smith,G.R. (2003) Nonrandom homolog segregation at meiosis I in *Schizosaccharomyces pombe* mutants lacking recombination. *Genetics*, **163**, 857–874.

8. Cromie,G.A., Hyppa,R.W., Taylor,A.F., Zakharyevich,K., Hunter,N. and Smith,G.R. (2006) Single Holliday junctions are intermediates of meiotic recombination. *Cell*, **127**, 1167–1178.
9. Hyppa,R.W. and Smith,G.R. (2010) Crossover invariance determined by partner choice for meiotic DNA break repair. *Cell*, **142**, 243–255.
10. Paques,F. and Haber,J.E. (1999) Multiple pathways of recombination induced by double-strand breaks in *Saccharomyces cerevisiae*. *Microbiol. Mol. Biol. Rev.*, **63**, 349–404.
11. Heyer,W.D., Ehmsen,K.T. and Liu,J. (2010) Regulation of homologous recombination in eukaryotes. *Annu. Rev. Genet.*, **44**, 113–139.
12. Hickson,I.D. and Mankouri,H.W. (2011) Processing of homologous recombination repair Intermediates by the Sgs1-Top3-Rmi1 and Mus81-Mms4 complexes. *Cell Cycle*, **10**, 3078–3085.
13. Roseaulin,L., Yamada,Y., Tsutsui,Y., Russell,P., Iwasaki,H. and Arcangioli,B. (2008) Mus81 is essential for sister chromatid recombination at broken replication forks. *EMBO J.*, **27**, 1378–1387.
14. Agmon,N., Yovel,M., Harari,Y., Liefshitz,B. and Kupiec,M. (2011) The role of Holliday junction resolvases in the repair of spontaneous and induced DNA damage. *Nucleic Acids Res.*, **39**, 7009–7019.
15. Boddy,M.N., Gaillard,P.H., McDonald,W.H., Shanahan,P., Yates,J.R. III and Russell,P. (2001) Mus81-Eme1 are essential components of a Holliday junction resolvase. *Cell*, **107**, 537–548.
16. Oh,S.D., Lao,J.P., Taylor,A.F., Smith,G.R. and Hunter,N. (2008) RecQ helicase, Sgs1, and XPF family endonuclease, Mus81-Mms4, resolve aberrant joint molecules during meiotic recombination. *Mol. Cell*, **31**, 324–336.
17. Jessop,L. and Lichten,M. (2008) Mus81/Mms4 endonuclease and Sgs1 helicase collaborate to ensure proper recombination intermediate metabolism during meiosis. *Mol. Cell*, **31**, 313–323.
18. Lorenz,A., West,S.C. and Whitby,M.C. (2010) The human Holliday junction resolvase GEN1 rescues the meiotic phenotype of a *Schizosaccharomyces pombe mus81* mutant. *Nucleic Acids Res.*, **38**, 1866–1873.
19. Matos,J., Blanco,M.G., Maslen,S., Skehel,J.M. and West,S.C. (2011) Regulatory control of the resolution of DNA recombination intermediates during meiosis and mitosis. *Cell*, **147**, 158–172.
20. Fekairi,S., Scaglione,S., Chahwan,C., Taylor,E.R., Tissier,A., Coulon,S., Dong,M.Q., Ruse,C., Yates,J.R. III, Russell,P. *et al.* (2009) Human SLX4 is a Holliday junction resolvase subunit that binds multiple DNA repair/recombination endonucleases. *Cell*, **138**, 78–89.
21. Svendsen,J.M., Smogorzewska,A., Sowa,M.E., O'Connell,B.C., Gygi,S.P., Elledge,S.J. and Harper,J.W. (2009) Mammalian BTBD12/SLX4 assembles a Holliday junction resolvase and is required for DNA repair. *Cell*, **138**, 63–77.
22. Schwartz,E.K. and Heyer,W.D. (2011) Processing of joint molecule intermediates by structure-selective endonucleases during homologous recombination in eukaryotes. *Chromosoma*, **120**, 109–127.
23. Osman,F., Dixon,J., Doe,C.L. and Whitby,M.C. (2003) Generating crossovers by resolution of nicked Holliday junctions: a role for Mus81-Eme1 in meiosis. *Mol. Cell*, **12**, 761–774.
24. Blais,V., Gao,H., Elwell,C.A., Boddy,M.N., Gaillard,P.H., Russell,P. and McGowan,C.H. (2004) RNA interference inhibition of Mus81 reduces mitotic recombination in human cells. *Mol. Biol. Cell*, **15**, 552–562.
25. Hope,J.C., Cruzata,L.D., Duvshani,A., Mitsumoto,J., Maftahi,M. and Freyer,G.A. (2007) Mus81-Eme1-dependent and -independent crossovers form in mitotic cells during double-strand break repair in *Schizosaccharomyces pombe*. *Mol. Cell Biol.*, **27**, 3828–3838.
26. Smith,G.R., Boddy,M.N., Shanahan,P. and Russell,P. (2003) Fission yeast Mus81·Eme1 Holliday junction resolvase is required for meiotic crossing over but not for gene conversion. *Genetics*, **165**, 2289–2293.
27. Fricke,W.M., Bastin-Shanower,S.A. and Brill,S.J. (2005) Substrate specificity of the *Saccharomyces cerevisiae* Mus81-Mms4 endonuclease. *DNA Repair (Amst)*, **4**, 243–251.
28. Ehmsen,K.T. and Heyer,W.D. (2008) *Saccharomyces cerevisiae* Mus81-Mms4 is a catalytic, DNA structure-selective endonuclease. *Nucleic Acids Res.*, **36**, 2182–2195.
29. Gaskell,L.J., Osman,F., Gilbert,R.J. and Whitby,M.C. (2007) Mus81 cleavage of Holliday junctions: a failsafe for processing meiotic recombination intermediates? *EMBO J*, **26**, 1891–1901.
30. Doe,C.L., Ahn,J.S., Dixon,J. and Whitby,M.C. (2002) Mus81-Eme1 and Rqh1 involvement in processing stalled and collapsed replication forks. *J. Biol. Chem.*, **277**, 32753–32759.
31. Bolt,E.L., Sharples,G.J. and Lloyd,R.G. (1999) Identification of three aspartic acid residues essential for catalysis by the RusA Holliday junction resolvase. *J. Mol. Biol.*, **286**, 403–415.
32. Mankouri,H.W., Ashton,T.M. and Hickson,I.D. (2011) Holliday junction-containing DNA structures persist in cells lacking Sgs1 or Top3 following exposure to DNA damage. *Proc. Natl. Acad. Sci. USA*, **108**, 4944–4949.
33. De Piccoli,G., Torres-Rosell,J. and Aragon,L. (2009) The unnamed complex: what do we know about Smc5-Smc6? *Chromosome Res.*, **17**, 251–263.
34. Doyle,J.M., Gao,J., Wang,J., Yang,M. and Potts,P.R. (2010) MAGE-RING protein complexes comprise a family of E3 ubiquitin ligases. *Mol. Cell*, **39**, 963–974.
35. Pebernard,S., Wohlschlegel,J., McDonald,W.H., Yates,J.R. III and Boddy,M.N. (2006) The Nse5-Nse6 dimer mediates DNA repair roles of the Smc5-Smc6 complex. *Mol. Cell Biol.*, **26**, 1617–1630.
36. Lindroos,H.B., Strom,L., Itoh,T., Katou,Y., Shirahige,K. and Sjogren,C. (2006) Chromosomal association of the Smc5/6 complex reveals that it functions in differently regulated pathways. *Mol. Cell*, **22**, 755–767.
37. De Piccoli,G., Cortes-Ledesma,F., Ira,G., Torres-Rosell,J., Uhle,S., Farmer,S., Hwang,J.Y., Machin,F., Ceschia,A., McAleenan,A. *et al.* (2006) Smc5-Smc6 mediate DNA double-strand-break repair by promoting sister-chromatid recombination. *Nat. Cell Biol.*, **8**, 1032–1034.
38. Potts,P.R., Porteus,M.H. and Yu,H. (2006) Human SMC5/6 complex promotes sister chromatid homologous recombination by recruiting the SMC1/3 cohesin complex to double-strand breaks. *EMBO J.*, **25**, 3377–3388.
39. Verkade,H.M., Bugg,S.J., Lindsay,H.D., Carr,A.M. and O'Connell,M.J. (1999) Rad18 is required for DNA repair and checkpoint responses in fission yeast. *Mol. Biol. Cell*, **10**, 2905–2918.
40. Harvey,S.H., Sheedy,D.M., Cuddihy,A.R. and O'Connell,M.J. (2004) Coordination of DNA damage responses via the Smc5/Smc6 complex. *Mol. Cell Biol.*, **24**, 662–674.
41. Lehmann,A.R. (2005) The role of SMC proteins in the responses to DNA damage. *DNA Repair (Amst)*, **4**, 309–314.
42. McDonald,W.H., Pavlova,Y., Yates,J.R. III and Boddy,M.N. (2003) Novel essential DNA repair proteins Nse1 and Nse2 are subunits of the fission yeast Smc5-Smc6 complex. *J. Biol. Chem.*, **278**, 45460–45467.
43. Morikawa,H., Morishita,T., Kawane,S., Iwasaki,H., Carr,A.M. and Shinagawa,H. (2004) Rad62 protein functionally and physically associates with the Smc5/Smc6 protein complex and is required for chromosome integrity and recombination repair in fission yeast. *Mol. Cell Biol.*, **24**, 9401–9413.
44. Kegel,A. and Sjögren,C. (2011) The Smc5/6 complex: more than repair? *Cold Spring Harb. Symp. Quant. Biol.*, **75**, 179–187.
45. Branzei,D., Sollier,J., Liberi,G., Zhao,X., Maeda,D., Seki,M., Enomoto,T., Ohta,K. and Foiani,M. (2006) Ubc9- and Mms21-mediated sumoylation counteracts recombinogenic events at damaged replication forks. *Cell*, **127**, 509–522.
46. Ampatzidou,E., Irmisch,A., O'Connell,M.J. and Murray,J.M. (2006) Smc5/6 is required for repair at collapsed replication forks. *Mol. Cell Biol.*, **26**, 9387–9401.
47. Bermudez-Lopez,M., Ceschia,A., de Piccoli,G., Colomina,N., Pasero,P., Aragon,L. and Torres-Rosell,J. (2010) The Smc5/6 complex is required for dissolution of DNA-mediated sister chromatid linkages. *Nucleic Acids Res.*, **38**, 6502–6512.
48. Chavez,A., Agrawal,V. and Johnson,F.B. (2011) Homologous recombination-dependent rescue of deficiency in the structural maintenance of chromosomes (Smc) 5/6 complex. *J. Biol. Chem.*, **286**, 5119–5125.
49. Chavez,A., George,V., Agrawal,V. and Johnson,F.B. (2010) Sumoylation and the structural maintenance of chromosomes

(Smc) 5/6 complex slow senescence through recombination intermediate resolution. *J. Biol. Chem.*, **285**, 11922–11930.
50. Chen,Y.H., Choi,K., Szakal,B., Arenz,J., Duan,X., Ye,H., Branzei,D. and Zhao,X. (2009) Interplay between the Smc5/6 complex and the Mph1 helicase in recombinational repair. *Proc. Natl. Acad. Sci. USA*, **106**, 21252–21257.
51. Choi,K., Szakal,B., Chen,Y.H., Branzei,D. and Zhao,X. (2010) The Smc5/6 complex and Esc2 influence multiple replication-associated recombination processes in *Saccharomyces cerevisiae*. *Mol. Biol. Cell*, **21**, 2306–2314.
52. Miyabe,I., Morishita,T., Hishida,T., Yonei,S. and Shinagawa,H. (2006) Rhp51-dependent recombination intermediates that do not generate checkpoint signal are accumulated in *Schizosaccharomyces pombe rad60* and *smc5/6* mutants after release from replication arrest. *Mol. Cell Biol.*, **26**, 343–353.
53. Sollier,J., Driscoll,R., Castellucci,F., Foiani,M., Jackson,S.P. and Branzei,D. (2009) The *Saccharomyces cerevisiae* Esc2 and Smc5-6 proteins promote sister chromatid junction-mediated intra-S repair. *Mol. Biol. Cell*, **20**, 1671–1682.
54. Torres-Rosell,J., Machin,F., Farmer,S., Jarmuz,A., Eydmann,T., Dalgaard,J.Z. and Aragon,L. (2005) SMC5 and SMC6 genes are required for the segregation of repetitive chromosome regions. *Nat. Cell Biol.*, **7**, 412–419.
55. Branzei,D., Vanoli,F. and Foiani,M. (2008) SUMOylation regulates Rad18-mediated template switch. *Nature*, **456**, 915–920.
56. Moreno,S., Klar,A. and Nurse,P. (1991) Molecular genetic analysis of fission yeast *Schizosaccharomyces pombe*. *Methods Enzymol.*, **194**, 795–823.
57. Prudden,J., Pebernard,S., Raffa,G., Slavin,D.A., Perry,J.J., Tainer,J.A., McGowan,C.H. and Boddy,M.N. (2007) SUMO-targeted ubiquitin ligases in genome stability. *EMBO J.*, **26**, 4089–4101.
58. Cullen,J.K., Hussey,S.P., Walker,C., Prudden,J., Wee,B.Y., Dave,A., Findlay,J.S., Savory,A.P. and Humphrey,T.C. (2007) Break-induced loss of heterozygosity in fission yeast: dual roles for homologous recombination in promoting translocations and preventing de novo telomere addition. *Mol. Cell Biol.*, **27**, 7745–7757.
59. Khasanov,F.K., Savchenko,G.V., Bashkirova,E.V., Korolev,V.G., Heyer,W.-D. and Bashkirov,V.I. (1999) A new recombinational DNA repair gene from *Schizosaccharomyces pombe* with homology to *Escherichia coli* RecA. *Genetics*, **152**, 1557–1572.
60. Lin,Y. and Smith,G.R. (1994) Transient, meiosis-induced expression of the *rec6* and *rec12* genes of *Schizosaccharomyces pombe*. *Genetics*, **136**, 769–779.
61. Cromie,G.A., Rubio,C.A., Hyppa,R.W. and Smith,G.R. (2005) A natural meiotic DNA break site in *Schizosaccharomyces pombe* is a hotspot of gene conversion, highly associated with crossing over. *Genetics*, **169**, 595–605.
62. Tatebe,H., Goshima,G., Takeda,K., Nakagawa,T., Kinoshita,K. and Yanagida,M. (2001) Fission yeast living mitosis visualized by GFP-tagged gene products. *Micron*, **32**, 67–74.
63. Sato,M., Dhut,S. and Toda,T. (2005) New drug-resistant cassettes for gene disruption and epitope tagging in *Schizosaccharomyces pombe*. *Yeast*, **22**, 583–591.
64. Bahler,J., Wu,J., Longtine,M.S., Shah,N.G., McKenzie,A., Steever,A.B., Wach,A., Phileppsen,P. and Pringle,J.R. (1998) Heterologous modules for efficient and versatile PCR-based gene targetting in *Schizosaccharomyces pombe*. *Yeast*, **14**, 943–951.
65. Davis,L., Rozalen,A.E., Moreno,S., Smith,G.R. and Martin-Castellanos,C. (2008) Rec25 and Rec27, novel linear-element components, link cohesin to meiotic DNA breakage and recombination. *Curr. Biol.*, **18**, 849–854.
66. Gutz,H., Heslot,H., Leupold,U. and Lopreno,N. (1974) In: King,R.C. (ed.), *Schizosaccharomyces pombe Handbook of Genetics*, Vol. 1. Plenum Press, New York, pp. 395–446.
67. De Veaux,L.C., Hoagland,N.A. and Smith,G.R. (1992) Seventeen complementation groups of mutations decreasing meiotic recombination in *Schizosaccharomyces pombe*. *Genetics*, **130**, 251–262.
68. Cervantes,M.D., Farah,J.A. and Smith,G.R. (2000) Meiotic DNA breaks associated with recombination in *S. pombe*. *Mol. Cell*, **5**, 883–888.
69. Young,J.A., Schreckhise,R.W., Steiner,W.W. and Smith,G.R. (2002) Meiotic recombination remote from prominent DNA break sites in *S. pombe*. *Mol. Cell*, **9**, 253–263.
70. Tinline-Purvis,H., Savory,A.P., Cullen,J.K., Dave,A., Moss,J., Bridge,W.L., Marguerat,S., Bahler,J., Ragoussis,J., Mott,R. *et al.* (2009) Failed gene conversion leads to extensive end processing and chromosomal rearrangements in fission yeast. *EMBO J.*, **28**, 3400–3412.
71. Boddy,M.N., Lopez-Girona,A., Shanahan,P., Interthal,H., Heyer,W.D. and Russell,P. (2000) Damage tolerance protein Mus81 associates with the FHA1 domain of checkpoint kinase Cds1. *Mol. Cell Biol.*, **20**, 8758–8766.
72. Doe,C.L., Dixon,J., Osman,F. and Whitby,M.C. (2000) Partial suppression of the fission yeast *rqh1*$^-$ phenotype by expression of a bacterial Holliday junction resolvase. *EMBO J.*, **19**, 2751–2762.
73. Young,J.A., Hyppa,R.W. and Smith,G.R. (2004) Conserved and nonconserved proteins for meiotic DNA breakage and repair in yeasts. *Genetics*, **167**, 593–605.
74. Cromie,G.A., Hyppa,R.W., Cam,H.P., Farah,J.A., Grewal,S.I. and Smith,G.R. (2007) A discrete class of intergenic DNA dictates meiotic DNA break hotspots in fission yeast. *PLoS Genet.*, **3**, e141.
75. Dunderdale,H.J., Sharples,G.J., Lloyd,R.G. and West,S.C. (1994) Cloning, overexpression, purification, and characterization of the *Escherichia coli* RuvC Holliday junction resolvase. *J. Biol. Chem.*, **269**, 5187–5194.
76. Liberi,G., Maffioletti,G., Lucca,C., Chiolo,I., Baryshnikova,A., Cotta-Ramusino,C., Lopes,M., Pellicioli,A., Haber,J.E. and Foiani,M. (2005) Rad51-dependent DNA structures accumulate at damaged replication forks in *sgs1* mutants defective in the yeast ortholog of BLM RecQ helicase. *Genes Dev.*, **19**, 339–350.
77. Bustard,D.E., Menolfi,D., Jeppsson,K., Ball,L.G., Dewey,S.C., Shirahige,K., Sjogren,C., Branzei,D. and Cobb,J.A. (2012) During replication stress Non-Smc-Element 5 is required for Smc5/6 complex functionality at stalled forks. *J. Biol. Chem.*, **287**, 11374–11383.
78. Robinson,N.P., Blood,K.A., McCallum,S.A., Edwards,P.A. and Bell,S.D. (2007) Sister chromatid junctions in the hyperthermophilic archaeon *Sulfolobus solfataricus*. *EMBO J.*, **26**, 816–824.
79. Kegel,A., Betts-Lindroos,H., Kanno,T., Jeppsson,K., Strom,L., Katou,Y., Itoh,T., Shirahige,K. and Sjogren,C. (2011) Chromosome length influences replication-induced topological stress. *Nature*, **471**, 392–396.
80. Andrews,E.A., Palecek,J., Sergeant,J., Taylor,E., Lehmann,A.R. and Watts,F.Z. (2005) Nse2, a component of the Smc5-6 complex, is a SUMO ligase required for the response to DNA damage. *Mol. Cell Biol.*, **25**, 185–196.
81. Pebernard,S., Perry,J.J., Tainer,J.A. and Boddy,M.N. (2008) Nse1 RING-like domain supports functions of the Smc5-Smc6 holocomplex in genome stability. *Mol. Biol. Cell*, **19**, 4099–4109.
82. Watts,F.Z., Skilton,A., Ho,J.C., Boyd,L.K., Trickey,M.A., Gardner,L., Ogi,F.X. and Outwin,E.A. (2007) The role of *Schizosaccharomyces pombe* SUMO ligases in genome stability. *Biochem. Soc. Trans.*, **35**, 1379–1384.
83. Pebernard,S., McDonald,W.H., Pavlova,Y., Yates,J.R. III and Boddy,M.N. (2004) Nse1, Nse2, and a novel subunit of the Smc5-Smc6 complex, Nse3, play a crucial role in meiosis. *Mol. Biol. Cell*, **15**, 4866–4876.
84. Farmer,S., San-Segundo,P.A. and Aragon,L. (2011) The Smc5-Smc6 complex is required to remove chromosome junctions in meiosis. *PLoS One*, **6**, e20948.
85. Munz,P. (1994) An analysis of interference in the fission yeast *Schizosaccharomyces pombe*. *Genetics*, **137**, 701–707.
86. Leupold. and Gutz. (1964) Genetic fine structure in *Schizosaccharomyces pombe*. *Proc IX Intl Congr Genet*, **2**, 31–35.
87. McLeod,M., Stein,M. and Beach,D.H. (1987) The product of the *mei3*$^+$ gene, expressed under the control of the mating type locus, induces meiosis and sporulation in fission yeast. *EMBO J.*, **6**, 729–736.
88. Brewer,B.J. and Fangman,W.L. (1987) The localization of replication origins on ARS plasmids in *S. cerevisiae*. *Cell*, **51**, 463–471.